

Ferroelectric effects in PZT

L. Bellaiche, J. Padilla and David Vanderbilt

Department of Physics and Astronomy, Rutgers University, Piscataway, New Jersey 08855-0849

Abstract. First-principles calculations are performed to investigate alloying and ferroelectric effects in lead zirconate titanate (PZT) with high Ti composition. We find that the main effect of alloying in the paraelectric phase of PZT is the existence of two sets of B–O bonds, i.e., shorter Ti–O bonds *vs.* longer Zr–O bonds. On the other hand, ferroelectricity leads to the formation of very short covalent Ti–O bonds and to the formation of covalent chains of Pb–O bonds. The covalency in the ferroelectric phase is mainly induced by an enhancement of hybridization between Ti $3d$ and O $2p$, and between Pb $6s$ and O $2p$. These hybridizations induce a striking decrease of the effective charges when going from the paraelectric to the ferroelectric phase of PZT.

INTRODUCTION

The technologically important lead zirconate titanate alloy (i.e., $\text{PbZr}_{1-x}\text{Ti}_x\text{O}_3$ usually denoted as PZT) has an interesting phase diagram [1]. Increasing the Ti x composition yields progressively the following *ground state* phases: an antiferroelectric orthorhombic phase for $x \lesssim 0.1$, a ferroelectric rhombohedral FE_2 phase for $0.1 \lesssim x \lesssim 0.4$, another ferroelectric rhombohedral FE_1 phase for $0.4 \lesssim x \lesssim 0.5$, and finally a tetragonal ferroelectric phase for x larger than 50%. The high-temperature phase of this alloy at all compositions is the cubic perovskite structure.

Previous theoretical studies [2] focused on the long-range B-site ordering effects in PZT for a Ti composition equal to 0.5, i.e., close to the morphotropic phase boundary between rhombohedral and tetragonal ferroelectric phases. The subject of the present theoretical study is rather different: we will investigate alloying and ferroelectric effects on structural, chemical and dielectric properties in the tetragonal phase of the PZT alloy. In other words, we would like to know what are the effects of alloying and ferroelectricity on bond lengths, chemical bonding and Born effective charges in PZT with high Ti content.

METHOD

We focus on the ordered structure shown in Fig. 1 and exhibiting a Ti composition equal to 2/3. The B-site ordering of this supercell consists of one Zr plane

alternating with two Ti planes along the [001] direction. We perform local-density approximation (LDA) calculations on this supercell using the Vanderbilt ultrasoft-pseudopotential scheme [3], and including the semicore shells for *all* the metals considered. Specifically, the Pb 5*d*, 6*s* and 6*p*, the Zr 4*s*, 4*p*, 4*d* and 5*s*, the Ti 3*s*, 3*p*, 3*d* and 4*s*, and the O 2*s* and 2*p* electrons are treated as valence electrons. We choose the plane-wave cutoff to be 25 Ry and use the Ceperley-Alder exchange and correlation [4] as parameterized by Perdew and Zunger [5]. The first-principles calculations throughout this work are performed using a (6,6,2) Monkhorst-Pack mesh [6]. Further technical details of the procedure used in the present study can be found in Ref. [7].

In fact, we perform two different calculations corresponding to two different symmetries of the structure shown in Fig. 1: (1) using a centrosymmetric cell (i.e., exhibiting an inversion symmetry about the central Pb atom); and (2) using a ferroelectric cell (i.e., relaxing the inversion symmetry constraint). Results of calculation (1) identify the alloying effects on various physical properties, while comparison of (1) with (2) allows us to isolate the ferroelectric effects on those properties.

The lattice parameter, the axial ratio c/a and the atomic positions along the [001] (compositional) direction are optimized in calculation (1) by minimizing the total energy and the Hellmann-Feynman forces, the latter being converged to within 0.02 eV/Å.

The ferroelectric experimental ground state of $\text{Pb}(\text{Zr}_{1/3}\text{Ti}_{2/3})\text{O}_3$ has the tetrag-

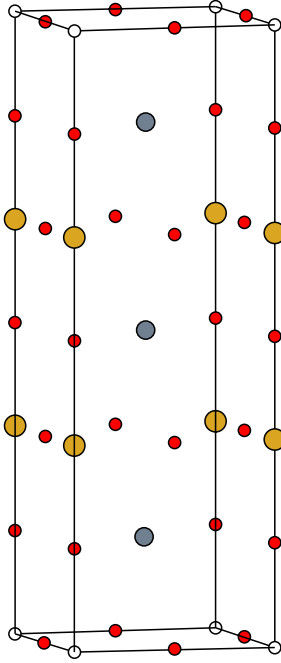


FIGURE 1. The [001]-ordered $\text{Pb}(\text{Zr}_{1/3}\text{Ti}_{2/3})\text{O}_3$ supercell. Tables I and II give the corresponding atomic positions in the paraelectric and ferroelectric phases.

onal P4mm point group and does not present any evidence of (long-range) B-site ordering. The material is thus composed of a succession of equivalent planes of composition $\text{Zr}_{1/3}\text{Ti}_{2/3}$ stacked along the tetragonal direction. To mimic this situation, we have chosen the ferroelectric direction in the supercell of Fig. 1 to lie along the [100] direction, rather than along the compositionally-modulated [001] direction. In our ferroelectric supercell, two axial ratios thus exist. These are the “ferroelectric-related” a_1/a and the “ordered-related” c/a , where a_1 , a , and c are the lengths of the supercell lattice vectors along the [100], [010], and [001] directions, respectively. We are thus dealing with a P2mm orthorhombic ferroelectric supercell rather than with a P4mm tetragonal ferroelectric supercell. However, in order to be as close as possible to the experimental situation, we will keep the c/a ratio as equal to the ideal value of 3. In this case, we shall refer to our ferroelectric cell as “quasi-tetragonal” along [100] (i.e., tetragonal as regards the axial ratios, although true tetragonal symmetry is broken down to orthorhombic by the B-plane ordering in the [001] direction). The lattice parameter a , the axial ratio a_1/a , and the atomic positions along the [100] and [001] directions are then optimized in calculation (2) by minimizing the total energy and the Hellmann-Feynman forces (again to within a tolerance of 0.02 eV/Å for the forces).

The determination of the electronic ground state in calculations (1) and (2) is used to investigate the ferroelectric effects on the bond length distribution and on the chemical bonding in PZT with high Ti content. The effective charges in each case (i.e., in both non-centrosymmetric and centrosymmetric cells) will then be calculated from the polarization differences between the ground state and slightly distorted structures, following the procedure introduced in Ref. [8] and intensively used in Ref. [9].

RESULTS

Centrosymmetric case

Optimizing each degree of freedom in the centrosymmetric supercell leads to the lattice vectors $\vec{a}_{1,c} = a_0[1, 0, 0]$, $\vec{a}_{2,c} = a_0[0, 1, 0]$, and $\vec{a}_{3,c} = a_0[0, 0, 2.99]$, where $a_0=7.498$ a.u. is the lattice parameter. The renormalized c/a ratio defined as the actual ratio (i.e., 2.99) divided by the ideal one (i.e., 3.00) is equal to 0.997 and is thus very close to unity. For this reason, our centrosymmetric supercell can be referred as “quasi-cubic”, which is consistent with the fact that the experimental paraelectric phase of PZT is cubic.

The relaxed atomic positions and the effective charges in this non-polar structure are given in Table I. It can be seen from Table I that (i) the Pb and O atoms lying between the Zr and Ti planes (i.e., Pb1, O1, Pb3, and O7) move significantly towards the Ti planes; and (ii) the Ti and O atoms belonging to the Ti planes (i.e., Ti1, O2, O3, Ti2, O5, and O6) move very slightly towards the central mirror (PbO) plane. These atomic motions lead to shortened Ti–O bonds and lengthened

TABLE 1. Structural relaxations and effective charges for the [001] centrosymmetric supercell. The Δz are the [001] atomic displacements of the non-polar structure with respect to the ideal ordered structure associated with $\vec{a}_{1,c}$, $\vec{a}_{2,c}$ and $\vec{a}_{3,c}$. Z_{xx} and Z_{zz} are the effective charges along the [100] and [001] direction, respectively.

Atoms	Relaxed positions			Displacements Δz (a.u.)	Effective charges	
	x (a.u.)	y (a.u.)	z (a.u.)		Z_{xx}	Z_{zz}
Pb1	3.749	3.749	-7.194	0.279	3.90	4.04
Pb2	3.749	3.749	0.000	0.000	3.88	3.53
Pb3	3.749	3.749	7.194	-0.279	3.90	4.04
Ti1	0.000	0.000	-3.643	0.093	6.77	6.65
Ti2	0.000	0.000	3.643	-0.093	6.77	6.65
Zr1	0.000	0.000	11.210	0.000	6.33	6.69
O1	0.000	0.000	-7.222	0.251	-2.58	-5.39
O2	3.749	0.000	-3.638	0.099	-5.58	-2.34
O3	0.000	3.749	-3.638	0.099	-2.72	-2.34
O4	0.000	0.000	0.000	0.000	-2.53	-5.57
O5	3.749	0.000	3.638	-0.099	-5.58	-2.34
O6	0.000	3.749	3.638	-0.099	-2.72	-2.34
O7	0.000	0.000	7.222	-0.251	-2.58	-5.39
O8	3.749	0.000	11.210	0.000	-5.17	-2.94
O9	0.000	3.749	11.210	0.000	-2.33	-2.94

Zr–O bonds. For example, the Ti1–O1 bond length shrinks to 1.89 Å, while Zr1–O7 enlarges to 2.11 Å, to be compared with the unrelaxed B–O bond length of 1.98 Å in the ideal structure. As a matter of fact, the appearance of several different bond lengths associated with the mixed sublattice seems to be a general feature of alloying, and has also been observed and predicted in zinc-blende, wurtzite and rocksalt alloys [10–15].

Alloying effects in the present ordered [001] structure also lead to a change in the lengths of the Pb–O bonds. For example, the Pb3–O bonds can be decomposed into three different groups: shorter Pb3–O bonds (e.g., Pb3–O5 equal to 2.73 Å), roughly unrelaxed Pb3–O bonds (e.g., Pb3–O7 equal to 2.80 Å), and long Pb3–O bonds (e.g., Pb3–O8 equal to 2.91 Å). The three groups are populated in the ratio 4:4:4. Thus, alloying has some significant effects on the B–O bonds ($\sim 4.5\%$ change in bond lengths), and to a smaller extent, on the Pb–O bonds ($\sim 2.5\%$ change).

The Born effective charges for our PZT supercell are detailed in Table I. They exhibit the same trends as in cubic bulk PbTiO_3 and PbZrO_3 compounds [9]: large values of about +4.0 for Pb atoms; large values around +6.5 for the B atoms; and two sets of values for the oxygen atoms, either close to -5.5 for oxygen atoms moving parallel to the B–O–B chain, or close to -2.5 for oxygen atoms moving perpendicular to these chains. The large values of the effective charges for B and O atoms are due to a (weak) hybridization between the B d and O $2p$ orbitals [9,16]. It is interesting to note that along the [001] axis, the effective charge of Ti is

TABLE 2. Structural relaxations and effective charges for the non-centrosymmetric supercell.

Atoms	Relaxed positions (a.u.)			Displacements (a.u.)			Effective charges	
	x	y	z	Δx	Δy	Δz	Z_{xx}	Z_{zz}
Pb1	3.547	3.731	-7.250	-0.334	0.000	0.211	3.17	3.92
Pb2	3.551	3.731	0.000	-0.331	0.000	0.000	3.37	3.56
Pb3	3.547	3.731	7.250	-0.334	0.000	-0.211	3.17	3.92
Ti1	0.015	0.000	-3.630	0.015	0.000	0.101	5.38	5.81
Ti2	0.015	0.000	3.630	0.015	0.000	-0.101	5.38	5.81
Zr1	0.118	0.000	11.192	0.118	0.000	0.000	6.06	6.06
O1	0.628	0.000	-7.223	0.628	0.000	0.238	-2.15	-4.80
O2	4.432	0.000	-3.637	0.551	0.000	0.094	-4.56	-1.95
O3	0.605	3.731	-3.634	0.605	0.000	0.097	-2.16	-2.59
O4	0.656	0.000	0.000	0.656	0.000	0.000	-2.10	-4.92
O5	4.432	0.000	3.637	0.551	0.000	-0.094	-4.56	-1.95
O6	0.605	3.731	3.634	0.605	0.000	0.097	-2.16	-2.59
O7	0.628	0.000	7.223	0.628	0.000	-0.238	-2.15	-4.80
O8	4.201	0.000	11.192	0.320	0.000	0.000	-4.62	-2.63
O9	0.779	3.731	11.192	0.779	0.000	0.000	-2.07	-2.90

very similar to that of Zr, while the difference between these two effective charges in the bulk parent compounds is larger than 1.0 (i.e., 7.06 *vs.* 5.85 for Ti and Zr respectively, according to Ref. [9]). One can also point out that the effective charge along [001] for atom O7 sitting between the Ti and Zr atoms is -5.39, i.e., very close to the average value -5.32 of the corresponding oxygen effective charges in the bulk parents (-5.83 and -4.81 for PbTiO₃ and PbZrO₃ respectively, according to Ref. [9]).

Ferroelectric effects

We now turn to a consideration of the *ferroelectric* effects on bond-length distributions and effective charges. Optimizing each degree of freedom in the non-centrosymmetric cell previously described yields the following lattice vectors in atomic units: $\vec{a}_{1,nc} = a'_0[1.040, 0, 0]$, $\vec{a}_{2,nc} = a'_0[0, 1, 0]$, and $\vec{a}_{3,nc} = a'_0[0, 0, 3.00]$, where the lattice parameter is $a'_0=7.461$ a.u., i.e., 0.5% smaller than for the centrosymmetric cell. A similar decrease of the lattice constant of around 0.7% has also been theoretically predicted when going from the paraelectric cubic phase to the tetragonal ferroelectric phase of the bulk PbTiO₃ compound [7,17]. By looking at $\vec{a}_{1,nc}$, we also notice that our calculation predicts a “ferroelectric-related” axial ratio a_1/a of 1.040. This prediction must be very close to the true value in Pb(Zr_{1/3}Ti_{2/3}), since recent measurements performed on Pb(Zr_{1-x}Ti_x) films [18] for $x=0.6$ found a value of 1.035 for this ratio, to be compared with values of 1.064 and 1.02 for $x = 1$ and $x \simeq 0.5$ respectively [1]. The optimized non-centrosymmetric cell has an energy that is 0.15 eV/5-atom-cell lower than that of the optimized centrosym-

metric cell. This is consistent with the fact that the experimental ground state of $\text{Pb}(\text{Zr}_{1/3}\text{Ti}_{2/3})$ is ferroelectric and tetragonal rather than paraelectric and cubic. The relaxed atomic positions and the effective charges in the non-centrosymmetric structure are shown in Table II. The quantities Δx , Δy , and Δz are the [100], [010] and [001] atomic displacements of the ferroelectric structure with respect to the ideal ordered structure associated with $\vec{a}_{1,nc}$, $\vec{a}_{2,nc}$ and $\vec{a}_{3,nc}$. Z_{xx} and Z_{zz} are the effective charges along the [100] and [001] directions, respectively.

A comparison of Tables I and II leads to the following observations. (i) The atomic displacements along the [001] direction are quite comparable between the centrosymmetric and the non-centrosymmetric phases. (ii) The ferroelectricity in tetragonal PZT is mainly characterized by the very large displacement of oxygen atoms along the tetragonal [100] direction (as in tetragonal PbTiO_3 bulk), the large displacement of Pb atoms along the $[\bar{1}00]$ direction, and by the slight displacement of Zr atoms along the [100] direction.

This ferroelectric atomic relaxation yields two different Ti–O bond lengths along the [100] direction: a very long bond of length 2.33 Å, which is even longer than the longest Zr–O bond (2.16 Å); and a very short bond of length 1.77 Å. This very short Ti–O bond is much shorter than the shortest Zr–O bond of 1.95 Å, and is of the same order as the shortest Ti–O bond of 1.78 Å occurring in tetragonal ferroelectric PbTiO_3 .

Ferroelectricity also leads to a drastic change in the Pb–O bonds. There are now some very short Pb–O bonds with an average length of 2.51 Å, “normal” Pb–O bonds with an average length of 2.84 Å, and very long Pb–O bonds with an average length of 3.26 Å. As in the centrosymmetric cell, the population ratio between these three groups is again 4:4:4. However, the oxygens exhibiting the shortest Pb–O bonds now share a common (100) plane, while they share a common (001) plane in the non-polar structure. Pair-distribution function analysis of recent pulsed neutron powder diffraction measurements on ferroelectric PZT alloys clearly confirms the existence of these three different groups [19]. The experimental average value of the three different Pb–O bond lengths is ~ 2.5 Å, ~ 2.9 Å, and ~ 3.4 Å, i.e., in excellent agreement with our predictions.

Comparing Table I and Table II also indicates that ferroelectricity leads to a striking decrease of the Born effective charges. The most spectacular decrease occurs for the atoms exhibiting a large change in their bond lengths. As a matter of fact, the effective charges along the [100] direction for atoms Ti1, Pb3 and O6 all decrease by $\sim 20\%$ with respect to the centrosymmetric case. In consequence, the effective charges of the Ti atoms and Pb atoms are reduced by 1.4 and 0.7, respectively, relative to their non-polar values. Previous theory has shown that a change of the effective charge by more than one unit of ‘e’ is indeed not unusual in going from the cubic to tetragonal ferroelectric phase in perovskite compounds [20,21]. The most extreme example appears to be for Nb in KNbO_3 , where the effective charges change from 9.67 to 7.05 in the direction parallel to the tetragonal axis.

To further understand the ferroelectric effects in PZT, Fig. 2 compares the

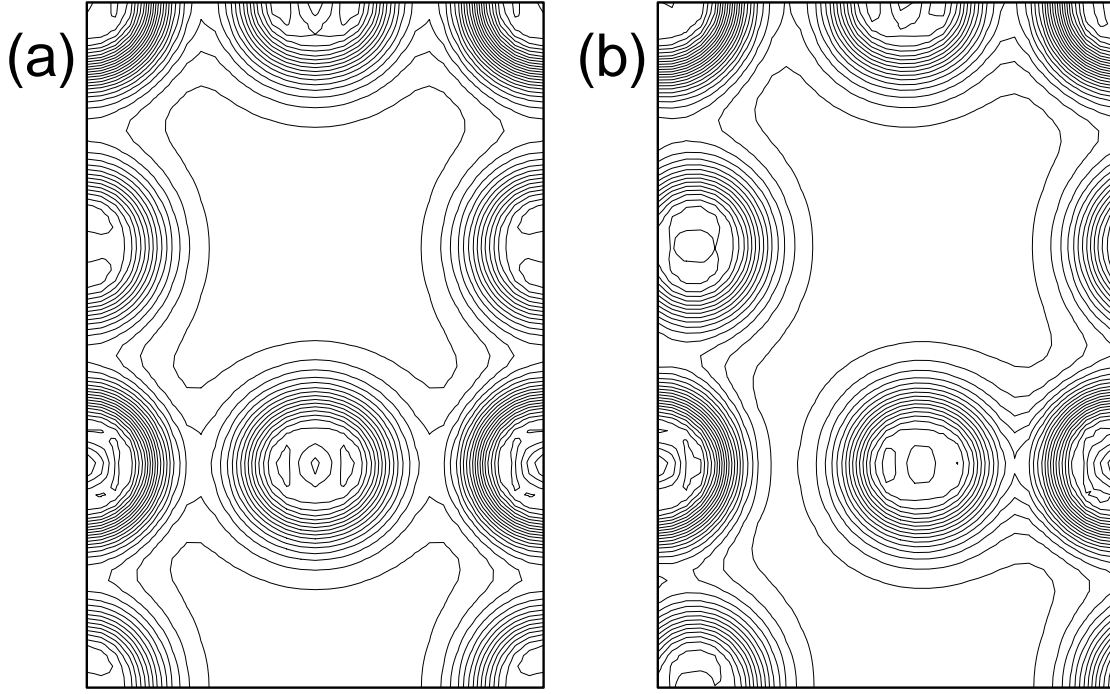


FIGURE 2. Electronic charge density plotted in the (B,O) plane for (a) paraelectric, and (b) ferroelectric, $\text{Pb}(\text{Zr}_{1/3}\text{Ti}_{2/3})\text{O}_3$ supercells. Only the upper half of the supercell is shown; the horizontal and vertical axes lie along $[100]$ and $[001]$ respectively. The sequence of atoms appearing at the left and right edges is Zr (top), O, Ti, O (bottom); and the remaining middle atoms are oxygens.

electronic charge density in the (B,O) planes for the centrosymmetric and non-centrosymmetric cases. Figure 3 shows a similar comparison but in the (Pb,O) planes. Figure 2 indicates that ferroelectricity in PZT leads (i) to a chemical breaking of some Ti–O bonds which generates the long Ti–O bonds of 2.33 Å, and (ii) to the formation of strong covalency between Ti and O, which is the cause of the very short Ti–O bonds of 1.77 Å. In fact, we also found similar behavior for the electronic charge density in the (Ti,O) plane for cubic and tetragonal lead titanate (PT). Thus, as in bulk PT [22], the formation of ferroelectricity in tetragonal PZT leads to an enhancement of hybridization between Ti 3*d* and O 2*p* orbitals. Interestingly, we don't observe in Fig. 2 any breaking of Zr–O bonds nor the formation of strong covalent Zr–O bonds. The different chemical behavior between Zr and Ti may perhaps be the cause of the difference in ground states exhibited by the corresponding bulk parents (antiferroelectric and orthorhombic for PbZrO_3 *vs.* ferroelectric and tetragonal for PbTiO_3). The striking feature of Fig. 3 is the formation of covalent chains between Pb and O atoms, which is the cause of the very short Pb–O bonds of 2.5 Å. We also found similar trends in the (Pb,O) planes

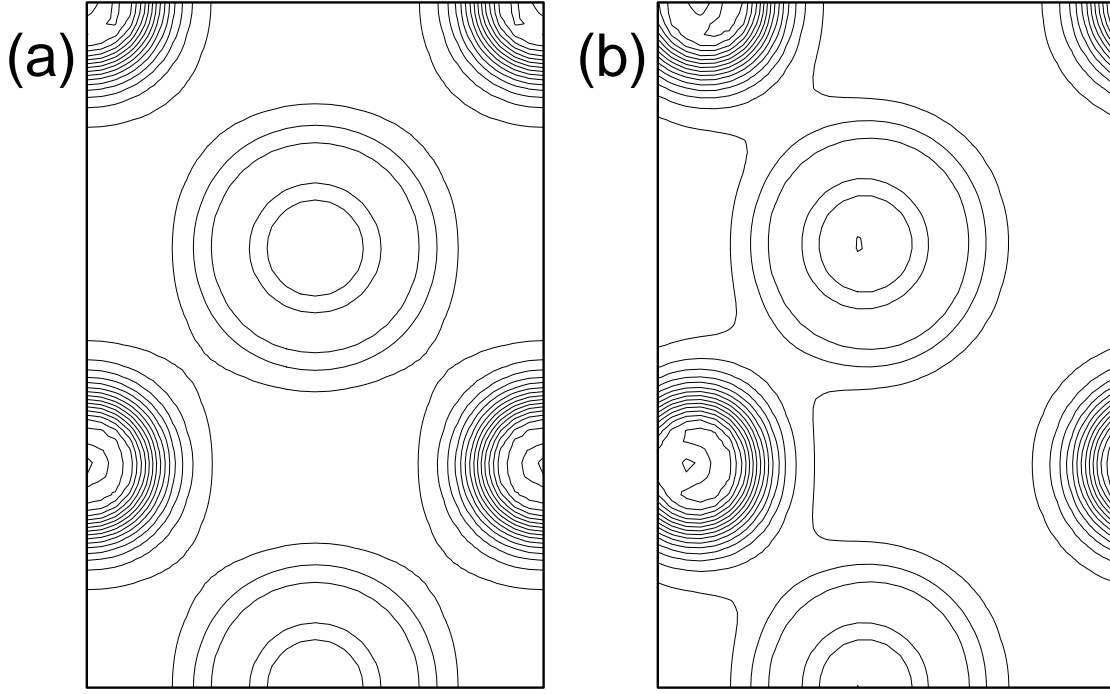


FIGURE 3. Electronic charge density plotted in the (Pb,O) plane for (a) paraelectric, and (b) ferroelectric, $\text{Pb}(\text{Zr}_{1/3}\text{Ti}_{2/3})\text{O}_3$ supercells. Only the upper half of the supercell is shown; the horizontal and vertical axes lie along $[100]$ and $[001]$ respectively. Atoms appearing at the left and right edges are O; atoms in the middle are Pb.

of paraelectric and ferroelectric PT. Thus, as in bulk PT [22], the hybridization between Pb 6s and O 2p orbitals plays an important role in the ferroelectric behavior of tetragonal PZT.

CONCLUSIONS

Using 15-atom supercells and Vanderbilt ultrasoft pseudopotentials within the local-density approximation, we investigated alloying and ferroelectric effects on the bond lengths, chemical bonding and effective charges in lead zirconate titanate alloys (PZT).

Our principal findings are as follows.

- (i) The centrosymmetric PZT alloy is mainly characterized by two sets of B–O bonds (shorter Ti–O bonds *vs.* longer Zr–O bonds), while the Pb–O bonds differ only slightly (by $\sim 2.5\%$) from the ideal structure.
- (ii) Allowing ferroelectricity in PZT alloys has two striking chemical effects: enhancement of hybridization between Ti 3d and O 2p orbitals, and hybridization between Pb 6s and O 2p orbitals.

(iii) These chemical and ferroelectric effects lead to the formation of very short covalent Ti–O bonds while breaking other Ti–O bonds, and give rise to the formation of covalent chains of very short Pb–O bonds.

(iv) The atoms engaged in covalent bonding exhibit a striking decrease of their effective charges by $\sim 20\%$ relative to the paraelectric phase.

ACKNOWLEDGMENTS

This work is supported by the Office of Naval Research grant N00014-97-1-0048. We thank Professor T. Egami for helpful discussions and for communicating his results with us.

REFERENCES

1. M.E. Lines and A.M. Glass, *Principles and Applications of Ferroelectrics and Related Materials* (Clarendon Press, Oxford, 1977).
2. G. Saghi-Szabo and R.E. Cohen, *Ferroelectrics* **194**, 287 (1997).
3. D. Vanderbilt, *Phys. Rev. B* **41**, 7892 (1990).
4. D.M. Ceperley and B.J. Alder *Phys. Rev. Lett.* **45**, 566 (1980).
5. J. Perdew and A. Zunger *Phys. Rev. B* **23**, 5048 (1981).
6. H.J. Monkhorst and J.D. Pack, *Phys. Rev. B* **13**, 5188 (1976).
7. R.D. King-Smith and D. Vanderbilt, *Phys. Rev. B* **49**, 5828 (1994).
8. R.D. King-Smith and D. Vanderbilt, *Phys. Rev. B* **47**, 1651 (1993).
9. W. Zhong, R.D. King-Smith and D. Vanderbilt, *Phys. Rev. Lett.* **72**, 3618 (1994).
10. J.C. Mikkelsen and J.B. Boyce, *Phys. Rev. Lett.* **49**, 1412 (1982).
11. Z. Wang and B.A. Bunker, *Phys. Rev. B* **46**, 11277 (1992).
12. J.L. Martins and A. Zunger, *Phys. Rev. B* **30**, 6217 (1984).
13. N. Marzari, S. de Gironcoli and S. Baroni, *Phys. Rev. Lett.* **72**, 4001 (1994).
14. C.K. Shih, W.E. Spicer, W.A. Harrison, and A. Sher, *Phys. Rev. B* **31**, 1139 (1985).
15. L. Bellaiche, S.H. Wei and A. Zunger *Phys. Rev. B* **56**, 13872 (1997).
16. M. Posternak, R. Resta and A. Baldereschi, *Phys. Rev. B* **50**, 8911 (1994).
17. A. Garcia and D. Vanderbilt, *Phys. Rev. B* **54**, 3817 (1996).
18. W. Zhu, Z.Q. Liu, W. Lu, M.S. Tse, H.S. Tan and X. Yao, *J. Appl. Phys.* **79**, 4283 (1996).
19. T. Egami, S. Teslic, W. Domowski, P.K. Davies and I.-W. Chen, *submitted* (1997).
20. Ph. Ghosez, X. Gonze, Ph. Lambin and J.-P. Michenaud *Phys. Rev. B* **51**, 6765 (1995).
21. C.-Z. Wang, R. Yu and H. Krakauer, *Phys. Rev. B* **54**, 11161 (1996).
22. R.E. Cohen, *Nature* **358**, 136 (1992).